Development of Foldable AMOLED Displays Based on Neutral-Plane Splitting Concept

Masumi Nishimura, Kisako Takebayashi, Masatomo Hishinuma, Hajime Yamaguchi, Akio Murayama

Research & Development Division, Japan Display Inc., 3300, Hayano, Mobara-shi, Chiba 297-8622 Japan
Keywords: Foldable display, Neutral-plane splitting, Bending stiffness, Adhesive, Organic light-emitting diode

ABSTRACT

Splitting of the mechanical neutral plane is a promising concept for foldable displays because it reduces the folding stress and stiffness of the display. We verified the concept experimentally and developed 5.5-inch full high-definition foldable AMOLED displays, which endured 150 k inward folding cycles with folding radius of 3 mm.

1 INTRODUCTION

The mobile communication devices should be both practical and portable. However, conforming to both the requirements is not always straightforward. Large displays are preferred for mobile devices; however, small displays are more portable. Foldable displays, which are size-adjustable, offer a promising solution to the portability-practicality trade-off.[1,2] Various displaying modes, such as electronic paper, liquid crystal, and organic light-emitting diodes (OLEDs), have been proposed for foldable displays.[3-5] The mobile device displays must also satisfy other specifications such as high-resolution, low-power consumption, light weight, thinness, durability, and flexible design. OLED displays are very promising because they have simple structures without backlight units and realize excellent image quality.[5-7]

The bending stress in a locality of a foldable display depends on the distance from the neutral mechanical plane, where the bending stress is zero (Figure 1). The bending stress in the multilayers is given by

$$\sigma = E_i \varepsilon \quad (1)$$

$$\varepsilon = (y - \lambda)/\rho \quad (2)$$

Here, σ, E_i, and ε denote the bending stress, elastic modulus of the i-th film in a certain module, and strain, respectively; y and λ are the positions of the target plane and the mechanically neutral plane, respectively; and ρ is the bending radius. The neutral plane position of a multilayered material is

$$\lambda = \sum_{i=1}^{n} E_i \left(h_i^{\,2} - h_{i-1}^{\,2}\right) / 2 \sum_{i=1}^{n} E_i t_i, \quad (3)$$

where h_i and t_i are the upper-surface position and thickness of the i-th layer, respectively, and $h_0 = 0$. There are two well-known methodologies for suppressing the bending stress. The first methodology is to reduce the display thickness. However, an OLED display usually has several functional films apart from the OLED panel. The other methodology is placing the neutral plane around a weak layer of the OLED display, such as the thin-film encapsulation (TFE) or thin-film transistor (TFT) layer, using additional films.[8,9] However, this solution must finely balance the functionality versus foldability trade-off.

The concept of neutral-plane splitting was proposed and theoretically studied as an alternative solution to this issue.[10,11] Figure 2 compares the display configurations of the neutral-plane splitting and the conventional neutral plane. The conventional configuration (Figure 2A) features one neutral plane of multilayers at the position given by Equation (3), whereas the neutral-plane split configuration (Figure 2B) possesses the plural neutral planes of multilayers. In neutral-plane splitting, the position of the neutral plane is determined in each film or submodule (collectively for some films), providing considerable freedom in designing a foldable OLED display.

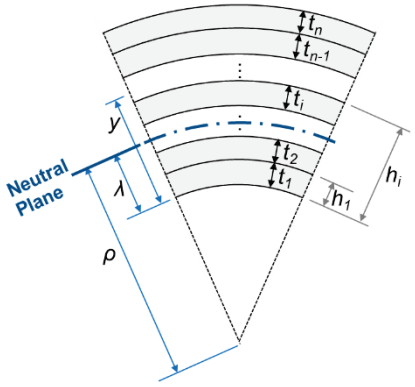

Figure 1. Schematic of a neutral plane of multilayers.

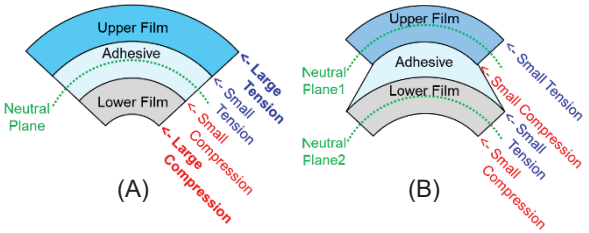

Figure 2. Schematic of neutral-pane splitting by an adhesive (cross-sectional view).
(A) Conventional folding (No splitting) and (B) This study (Perfect splitting). (A) has single neutral plane, but (B) has plural neutral planes.

In addition, the bending stiffness is reduced with neutral-plane splitting. Generally, conventional bending stiffness K_B in the multilayers is given by

$$K_B = \frac{b}{3}\sum_{i=1}^{n} E_i\{(h_i - \lambda)^3 - (h_{i-1} - \lambda)^3\}, \quad (4)$$

where b is the breadth of multilayers. According to equation (4), neutral-plane splitting decreases the bending stiffness because each layer has each neutral plane.

This report experimentally not only validates the concept of neutral-plane splitting on test samples,[12] but also shows that neutral-plane splitting reduces the bending stiffness. On the basis of this concept, we successfully develop 5.5-inch full high-definition (HD) 401-ppi foldable active matrix OLED (AMOLED) displays.

2 EXPERIMENT

Figure 3 is a schematic of the test sample used for verifying the neutral-plane splitting. Thin indium tin oxide (ITO) traces (30 loops) were formed on a 16 μm-thick polyimide (PI) substrate and covered with 0.2 μm-thick silicon nitride (SiN_x). When the test sample was folded, the SiN_x cracks caused disconnection of the trace loops, which was detected through electrical resistance measurements. We evaluated various modules: (a) the test sample only, (b) test samples stacked on simulated 50 μm-thick functional films (PI) using different adhesives, and (c) simulated 50 μm-thick functional films (poly-ethylene terephthalate; PET) stacked on other PET films using adhesives (Figure 4). Module (c) is used for the bending stiffness test. The elastic moduli of adhesives A, B, and C were E_a = 5000 kPa, E_b = 433 kPa, and E_c = 38 kPa, respectively.

Figure 5 shows a cross-sectional view of the equipment used in the folding evaluation. A module was set on the stage and folded by compression under the plate. The folding radius was defined as half the gap between the plate and the stage. In the bending stiffness test, a digital force gauge is attached to the plate, and the applied force for bending is measured to evaluate the bending stiffness, which the applied force is proportional to.

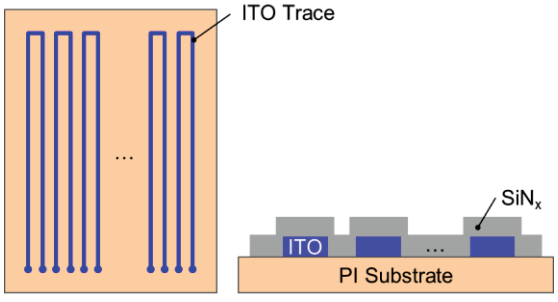

Figure 3. Schematics of test sample

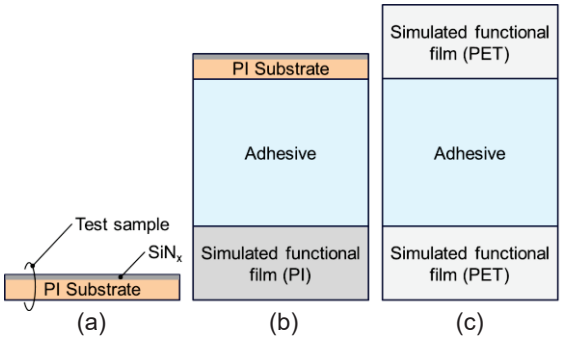

Figure 4. Schematic representations of the test modules: (a) test sample only, (b) test sample stacked on a simulated functional film by adhesives, and (c) a simulated functional film stacked on another simulated functional film by adhesives.

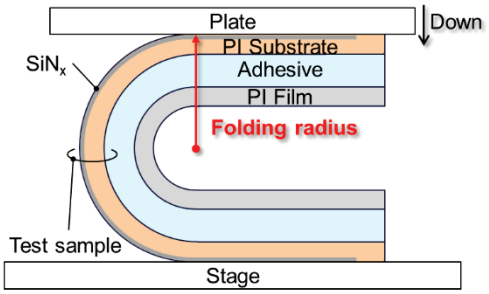

Figure 5. Cross-sectional view of the evaluation equipment.

3 RESULTS and DISCUSSION

3.1 Experimental verification of the neutral-plane splitting effect to the breaking bending radius

3.1.1 Test sample only

In this subsection, we evaluate the test sample only. When folded with the SiN_x layer facing outward, the traces of the test sample were disconnected at a folding radius of 0.8 mm. In this folding configuration, the SiN_x layer received the tensile strain. The tensile strain of SiN_x at breaking point (called the breaking strain of SiN_x) was calculated as 0.9% by Equation (2). On the other hand, when folded with the SiN_x layer facing inward, the traces were disconnected at a folding radius of 0.1 mm. In this folding configuration, the SiN_x received the compressive strain. The breaking compressive strain of SiN_x was calculated as 7.1% by Equation (2).

3.1.2 Test sample stacked on film with adhesive

In this subsection, we evaluate the test samples stacked on simulated functional films by various adhesives (module (b)). The test samples were folded with the SiN_x surface facing outward.

Figure 6 shows the folding-evaluation results of module b. The horizontal axis is the folding radius when all trace loops of the test sample become disconnected. If the neutral-plane splitting is perfect, as shown in Figure 2B, then all traces will be disconnected at a folding radius

of 0.8 mm, as found in module (a). On the other hand, if no neutral-plane splitting occurs, the traces should be disconnected at a folding radius of 10.4 mm. This calculation is based on Equation (2), where y, ε, and λ are the outer plane position, the breaking strain of SiN_x (0.9% as described in Section 3.1.1) and the neutral-plane position calculated by Equation (3), respectively. The traces of the test samples glued with adhesives A, B, and C were disconnected at folding radii of 4.7, 2.8, and 1.2 mm, respectively. These experimental results clearly show that all adhesives realize neutral-plane splitting and that adhesive C achieves nearly perfect splitting.

Figure 7 shows the relationship between the adhesive's elastic modulus and the position of the neutral plane in each test sample. The relative position of the neutral plane is plotted as the logarithm of the modulus. The neutral-plane position of the test samples was calculated by Equation (2). The folding radii ρ at the breaking points of the samples glued with different adhesives, along with the no-splitting and perfect-splitting cases, are compared in Figure 7. The relative neutral-plane positions were 0.45 with no splitting, 0.75, 0.86, and 0.93 with adhesives A, B, and C, respectively, and 0.96 with perfect splitting. Note that in the specimen glued with adhesive C, the neutral

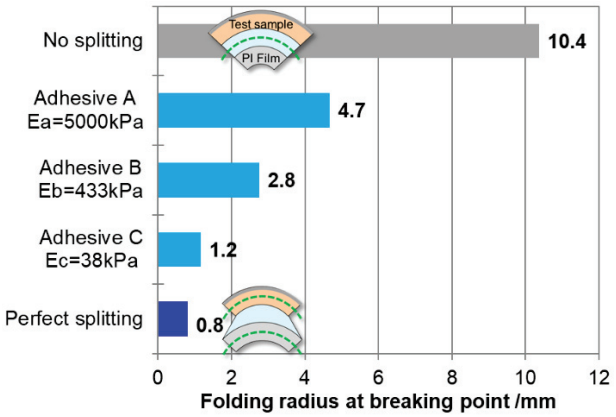

Figure 6. Folding radius at breaking point.

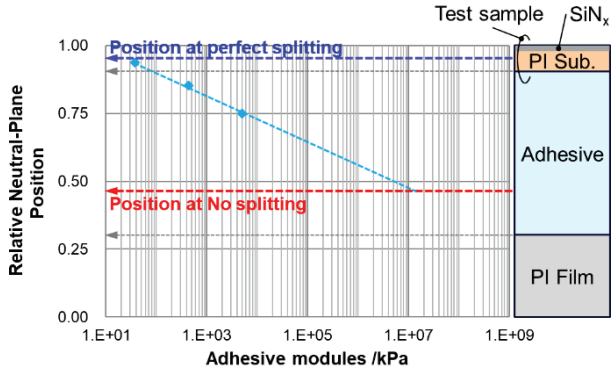

Figure 7. Relative position of neutral plane versus adhesive modulus (logarithmic scale) of the test samples. The relative total thickness of the module, including the test sample, adhesive and simulated functional film (PI), is defined as 1.0.

plane located inside the test sample despite the adhesives of the straight line and the no-splitting attachment of the simulated functional film. In Figure 7, the three points corresponding to the specimens glued with line is between several hundreds of MPa and a few GPa, close to the modulus of PI (the substrate of the simulated functional film and test sample). This result is reasonable because no splitting can occur when all layers have similar elastic moduli.

We demonstrated experimentally that the neutral-plane splitting is nearly perfect when the adhesive joining the substrate and the functional film has a low elastic modulus (in this case, 38 kPa), allowing larger deformation.

3.2 Experimental verification of the neutral-plane splitting effect to reduce the bending stiffness

The neutral-plane splitting affects the bending stiffness of foldable display. In this subsection, we evaluate simulated functional films (PET) stacked on other PET films using adhesive C, which is selected by evaluating test samples bonded with different adhesives as described above, (module (c)).

Figure 8 shows the evaluation results of the bending stiffness. The horizontal axis is the relative force for bending with 4-mm radius. The evaluated configurations are two 50 μm-thick PET films stacked with no adhesive, two 50 μm-thick PET films glued with adhesive C, and one 100 μm-thick PET film, which have the same total thickness of two 50 μm-thick PET films. One 100 μm-thick film showed the 3.62 times the force of two 50 μm-thick films stacked with no adhesive. However, two 50 μm-thick films glued with adhesive C has only 1.43 times the force. One 100 μm-thick film is equivalent to no splitting configuration, and two stacked films with no adhesive is equal to perfect splitting for two 50 μm-thick films glued with adhesive. Therefore, the bending stiffness of two films glued with adhesive C is much smaller than that at no splitting, and close to that at perfect splitting.

We demonstrated experimentally that the neutral-plane splitting reduces the bending stiffness when the adhesive joining films has a low elastic modulus.

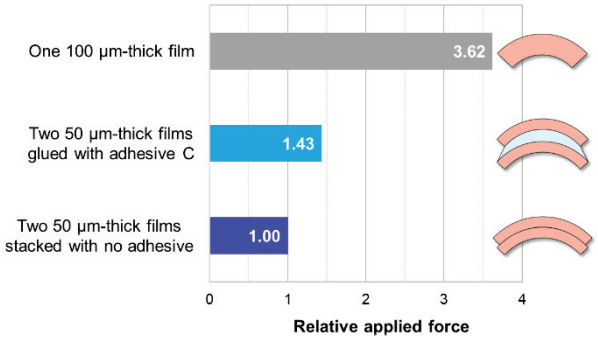

Figure 8. the repellent force against bending with 4-mm radius. The relative force of two 50 μm-thick films is defined as 1.0.

3.3 Fabrication and evaluation of foldable display prototypes

Finally, we constructed 5.5-inch full HD foldable AMOLED displays (see Figure 9 and Table 1). The display consists of an AMOLED panel and a circular polarizer. First, a low-temperature polycrystalline silicon TFT backplane was fabricated on a PI film formed on a glass substrate. A top-emission OLED and TFE were then fabricated on the backplane. The AMOLED panel was debonded from the glass substrate by the laser lift off technique. The polarizer was stacked on the panel with adhesive C, selected by evaluating test samples bonded with different adhesives as described above. Repeated folding tests were conducted with the apparatus which folds the sample without applying any tensile stress other than folding. Two sides of the AMOLED display were fixed at the ends of two subplates, which were moved to achieve the desired bending radius of the display. The prototype endured 150 k bending cycles with a 5-mm out -folding radius and a 3-mm in-folding radius. During out-folding and in-folding, the screen was located outside and inside of the prototype, respectively. To decide whether our prototype endured the cyclic folding, we checked for consistent performance and appearance of the display before and after folding. That is, the folding should not generate any dark spots, line defects, or bright dots.

4 CONCLUSIONS

We experimentally verified the concept of neutral-plane splitting. The relative position of the neutral plane was linearly related to the logarithm of the adhesive's elastic modulus and approached perfect splitting as the elastic modulus decreased.

Additionally, we experimentally showed neutral-plane splitting reduces the bending stiffness dramatically. The stiffness of the films glued with low elastic modulus decrease to approximately 40 % of stiffness when no splitting case occurs.

Using the selected adhesive based on the neutral-plane splitting concept, we then developed 5.5-inch full HD 401-ppi foldable AMOLED displays, which endures 150 k cyclic operations with out-folding and in-folding radii of 5 and 3 mm, respectively. We believe that this study will improve the flexibility of designing foldable AMOLED displays.

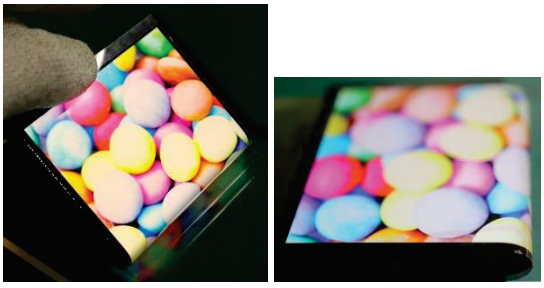

Figure 9. Prototype of the foldable AMOLED display during outward folding with a radius of 5 mm.

Table 1. Specifications of the foldable AMOLED display.

	Specifications
Display size	5.5 inch
Pixels	full HD (1080 × 1920)
Resolution	401ppi
Substrate	Polyimide
In-folding	R3 mm (150 k times)
Out-folding	R5 mm (150 k times)

5 ACKNOWLEDGEMENT

This paper is based on results obtained from a project subsidized by the New Energy and Industrial Technology Development Organization (NEDO).

REFERENCES

[1] Y. Jimbo, et al., “Tri-Fold Flexible AMOLED with High Barrier Passivation Layers,” SID Symp. Digest 45, 322–325 (2014).

[2] R. Komatsu, et al., “Repeatedly Foldable Book-Type AMOLED Display,” SID Symp. Digest 45, 326–329 (2014).

[3] E. Huitema, et al., “Flexible Electronic-Paper Active-Matrix Displays,” J. Soc. Info. Disp. 13/3, 181–185 (2005).

[4] T. Ishinabe, et al., “Substrate and Polymer-Wall Technologies for Future Foldable LCD Applications,” Proc. IDW 16, 91–94 (2016).

[5] M. Noda, et al., “Oxide TFTs and Color Filter Array Technology for Flexible Top-emission White OLED Display,” SID Symp. Digest 43, 998–1001 (2012).

[6] S. An, et al., “2.8-inch WQVGA Flexible AMOLED Using High Performance Low Temperature Polysilicon TFT on Plastic Substrates,” SID Symp. Digest 41, 706–709 (2010).

[7] H. Yamaguchi, et al., “11.7-inch Flexible AMOLED Display Driven by a-IGZO TFTs on Plastic Substrate,” SID Symp. Digest 43, 1002–1005 (2012).

[8] D.-U. Jin, et al. “Highly Robust Flexible AMOLED Display on Plastic Substrate with New Structure”, SID Symp. Digest 47, 703–705 (2010).

[9] C.-C. Lee, et al., “Flexibility Improvement of Foldable AMOLED with Touch Panel,” SID Symp. Digest 46, 238–241 (2015).

[10] Y. Su, et al., “Splitting of Neutral Mechanical Plane of Conformal, Multilayer Piezoelectric Mechanical Energy Harvester,” Appl. Phys. Lett. 107 041905 (2015).

[11] F. Salmon, et.al., “Modeling the Mechanical Performance of a Foldable Display Panel Bonded by 3M Optically Clear Adhesives,” SID Symp. Digest 48, 938–941 (2017).

[12] M. Nishimura, et al., “A 5.5-inch full HD foldable AMOLED display based on neutral-plane splitting concept,” J. Soc. Info. Disp. 27, 480–486 (2019).